Nonlinear optical properties of stimulated Brillouin scattering process in submerged object detection

Yuelan Lü (吕月兰), Lihua Wu (武立华), and Xueqing Chong (崇学庆)

College of Science, Harbin Engineering University, Harbin 150001

Received March 9, 2007

Nonlinear optical properties of stimulated Brillouin scattering (SBS) to signal detection in water are analyzed. With the threshold characteristics, SBS only occurs when the high power laser is focused in the SBS cell. When there is an object present in front of the focus, it leads to lower incident intensity and then SBS does not occur. The backward SBS signal depends on the focusing location. The nonlinear optical properties of SBS process in the focusing regime are analyzed theoretically. With the object coming near to the focusing center, the backward Stokes signal rises up from zero to a maximum, and then grows to saturation. The delay time of the echo signal to pump signal can give the object location. In experiment, the peak position of varying rate of energy can give object location.

OCIS codes: 010.3640, 190.5890, 140.3580, 140.7300.

People have made embedded studies on light dispersion technology as a method of ocean detection since the mid-1960s[1]. In this area, measurements have been performed for parameters such as velocity of sound, temperature, salinity, and coefficient of viscosity of the seawater mainly using Brillouin scattering[2−7]. Using injected mode-locked pulse laser and high accuracy scanning Fabry-Perot (F-P) interferometer, Fry *et al.* obtained Brillouin scattering spectrum that almost reached the theoretical limit[6]. On the basis of spontaneous Brillouin scattering in water, Gong *et al.*[8,9] put forward the submerged object detection technology based on spontaneous Brillouin scattering, whose basic idea is to determine the location of the object by the disappearance of the spontaneous Brillouin scattering signal in the water. However, because the spontaneous Brillouin scattering signal is very weak, the detection distance is not very long, and the system of the edge technique used is complicated[10]. This method has some difficulties in practical applications.

The feasibility of submerged object detection by focusing center in stimulated Brillouin scattering (SBS) process is proposed in this paper. The inflexion rate of Stokes signal is used to determine the location of the submerged object. In this way, we can get stronger echo signal and longer measurable distance.

The theoretical models are set up to describe the pulse propagation by the numerical solution of the three-dimensional (3D) coupling equations, including Maxwell wave equations and medium's energy transport equations. Under the condition of slowly varying envelope approximation, the 3D transient SBS equations can be simplified by three one-dimensional (1D) equations[11−14]. In a SBS medium, the nonlinear SBS process resonantly couples through electric-strain which produces an acoustic field in the medium. Thus a back-scattering Stokes field $A_{\rm s}(z,t)$ is built from the excited acoustic field $f(z,t)$, which is a theoretical model including the spontaneous nature of the initiation of SBS[8]. Energy is transported by the acoustic wave. Neglecting the acoustic propagation and the optical Kerr effect, we can obtain the slowly varying envelope approximation for the complex amplitudes. The equations are used to simulate SBS process as follows:

$$\left[\frac{n}{c}\left(\frac{\partial}{\partial t}\right)+\frac{\partial}{\partial z}\right]A_{\rm l}=-\alpha A_{\rm l}+ik\rho A_{\rm s}, \tag{1}$$

$$\left[\frac{n}{c}\left(\frac{\partial}{\partial t}\right)+\frac{\partial}{\partial z}\right]A_{\rm s}=\alpha A_{\rm s}-ik\rho^{*}A_{\rm l}, \tag{2}$$

$$\frac{\partial\rho}{\partial t}+\frac{\Gamma}{2}\rho=i\Lambda A_{\rm l}A_{\rm s}^{*}+f, \tag{3}$$

where n is the effective refraction index, c is the velocity of light, $\rho(z,t)$ is the density of medium, Γ is the damping rate of acoustic field, k, Λ are SBS coupled coefficients, $A_{\rm l}$ is the amplitude of pump laser.

A SBS process is suggested to be initiated by thermal noise $f(z,t)$, which exists in the end of water and can be amplified to build Stokes field. Based on the theoretical model of SBS initiated by one end noise thermal field, we introduced the initiated condition of the Gaussian random process as an equal distribution of noise field all through water. The coupled equations (1) − (3) can be solved by using an implicit finite difference in time and a backward differential scheme in space, which greatly reduces the computer's calculating time with separating time and space domain. In order to gain this procedure, the pulse is divided into small time intervals with the time increment assumed constant, and then the difference forms of coupled wave equations are established[15]. By an efficient numerical algorithm, a quasi-transient numerical simulation is formed. SBS process is built up in which dynamic properties of backward reflected SBS can be shown. In the above simulation, SBS parameters of water are adopted as follows. The absorption coefficient $\alpha=0.05$ cm^{-1}, the effective refraction index $n=1.324$, density $\rho=0.997$ g/cm^3, gain $g=3.8$ cm/GW, lifetime $\tau=1.87$ ns, $k=\frac{\gamma^{\rm e}\omega_{\rm L}}{4cn\rho_0}$, $\Lambda=\frac{\gamma^{\rm e}K^2}{16\pi\omega}$, $\gamma^{\rm e}$ is the electrostriction coefficient, ρ_0 is the average density of SBS media, K is the temperature, $\omega_{\rm L}$ is the laser frequency, and ω is the Stokes frequency. The initial laser field (laser pulses are input at $z=L$, the end

of the SBS cell) is known. We assumed quasi-Gaussian spatial and temporal intensity profiles of the incident laser pulse, which are closely matched with the intensity profiles of the laser pulses used in our experiments. Stokes field is built up from random noise field $f(z,t)$ whose shape is suggested Gaussian and configuration varies stochastic from 0 to 2π. Temporal and spatial boundary condition and initiated condition of the pump laser power are given. Then numerical solutions are presented under above conditions.

Since the phenomenon of the phase conjugation was discovered[16], this technology has been extensively studied. Different from the spontaneous Brillouin scattering, the elastic sound wave field in the process of SBS is produced by the electrostriction effects between SBS medium and incident laser field. This is a coherent sound wave field, which couples with the incident laser and produces SBS coherent radiation. It will obtain absolute success in contest with incoherent scattering and reflecting light. When the incident laser reaches SBS threshold, SBS occurs and most of incident laser energy will be translated into the Stokes wave which transmits backward. The most remarkable characteristic of SBS is its phase conjugation characteristic[10,11], i.e., the Stokes wave that transmits backward will follow the original path and its phase is just reversal of the pump pulse. The relationship of energy reflection dependent upon physical parameters is calculated by computer simulation. For the practical purpose, optical detection method can be controlled, so more attention is paid to the dependence of energy reflection on SBS focusing geometry with different pump powers. The theoretical simulation results for different pump energies with certain focusing geometry are shown in Fig. 1(a). Because the focal length is given, effective interaction length is fixed at a value within this focusing regime. When the object is just close to the focusing region from vicinity, the incident intensity increases quickly and reaches SBS threshold, SBS occurs and echo signal will be weak. When the object comes into the focusing region, incident intensity excesses SBS threshold, SBS begins to enhance, and then more and more energy of pump laser will be translated into backward Stokes wave and the reflected energy increases sharply. When the object goes out of focusing regime, the pump pulse is extracted, leading to the saturation of Stokes field[17]. So we can find the highest backward reflected energy. On the other hand, when the object comes out of the focusing regime in the near field, SBS disappears in the end. The curves in Fig. 1(a) all keep the same rule. Figure 1(b) shows the derivatives of Fig. 1(a). Position of submerged object can be determined by the maximum inflexion of varying energy of backward Stokes in theory. With the effective interaction length increasing, the Stokes field quickly gets strong with the increase of object location and then the rate of Stokes energy increases too; until the location of object comes to a point in which the energy Stokes field turns to decrease, the point should be the center of focusing length. For Fig. 1(b), the inflexion position ($L = 26$ cm) shows the location of object, which agrees with the focal length in water ($L = nF$, n is refractive index in water, F is the focal length in air). At the same time, the delay time of the echo signal to pump signal can be detected and give the distance of the submerged object. This method is very simple and can be easily brought into practice. The reflected energy variation with respect to the focal length is also explored. The focal length affects the SBS performance by changing the laser pulse beam radius. When the focal length is becoming longer, the laser beam radius increases sharply and the intensity of input laser pulses decreases, the corresponding pump energy threshold should rise up rapidly, and the detection error performance increases later. According to theoretical simulations, the shorter the SBS cell is, the shorter the location and the longer the focal length will be, thus the higher pump energy will be needed.

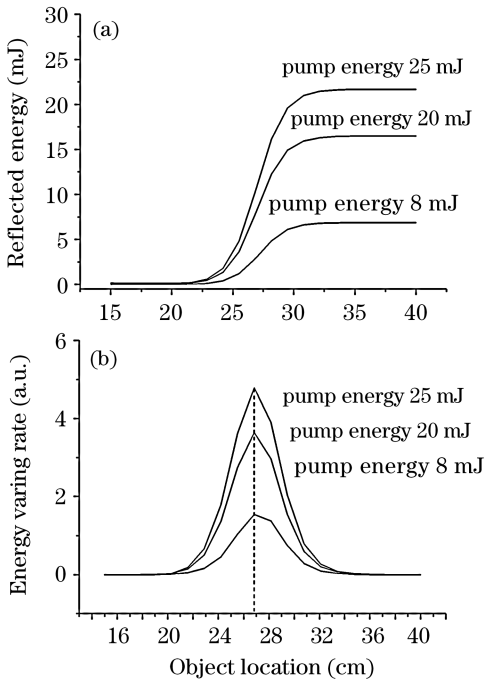

Fig. 1. Simulation of reflected energy dependent on the object location for different pump energies.

SBS only occurs when the laser power is above SBS threshold. Therefore, when laser is focused in water and its power density at the focus reaches the threshold, SBS will occur and part of the pump beam will be translated into the Stokes wave that transmits backward. However, when there is an object present in front of the focus, the laser cannot be focused, the incident intensity is less than SBS threshold, and SBS will not occur. The schematic diagram of detection is shown in Fig. 2. It consists of several parts: the pulse laser, the pre-extender system, the signal extracting system, the emission/reception

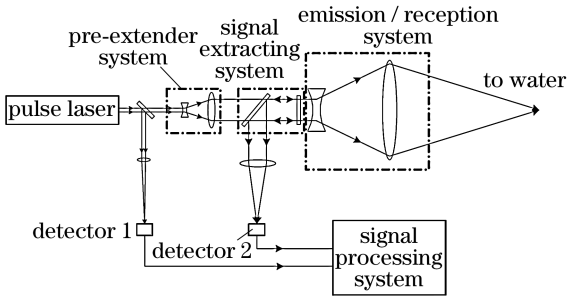

Fig. 2. Experimental setup.

system, and the signal processing system. The principle of detection is as follows. The pulse laser passes through the splitter, emerging from part of the pulse laser enters detector 1. The transmitted laser enters the pre-extender system, after which its power density decreases, therefore the subsequent signal extracting system can carry larger pulse energy; hence the detecting distance can be increased. The signal extracting system, through which the pulse laser enters the emission system, is used to extract backward Stokes signal. The emission system is a varying focal length emission device, whose focal length can be scanned from zero to a far distance. When there is not any object in front of the focus, SBS can occur. Because of the phase conjugation characteristic of SBS, the reflected Stokes wave will return along the original path. At this time, the former emission system turns into the reception system, and the Stokes wave is detected by detector 2 after being extracted. When the focus is scanning on the object, because the length of the SBS interaction becomes shorter, the intensity of the reflected Stokes wave reduces gradually, and after the focus has scanned the object, the Stokes wave will totally decrease sharply. At the same time, the waveforms of the pump beam and the Stokes wave which is beginning to decrease are recorded by detectors 1 and 2, and the delay time between the two waves is analyzed by the signal processing system, therefore the location of the object can be calculated.

For certain focusing geometry, the blue and green laser (450 − 570 nm) has little transmission loss and the strongest penetrating power in water. Therefore, we used a frequency-doubled Nd:YAG laser with an output wavelength of 532 nm, a Q-switched output pulse width of 7 ns and a single-pulse energy of 20 mJ. Because the single-pulse energy in the experiment was small, the pre-extender system was not used. The signal extracting system consisted of a polarizer and a 1/4 wave plate. The principle of signal extracting is that the polarization states of the pump pulse and the Stokes wave rotate by 90° after they pass through the 1/4 wave plate twice, so when the Stokes wave arrives at the polarizer for the second time, reflection will occur instead of transmission. The emission and reception system consisted of a combination of lens, whose focal length can be changed by adjusting the distance between the convex and the minus lens. The length of the flume used in the experiment was 2 m, and an object can be placed within $0-2$ m. A fast-response PIN tube was used in the experiment to detect the waveform of the pump pulse and the Stokes wave synchronously, and a TDS 3032B oscilloscope with 25-GS/s sampling rate was used to record the waveform.

For certain focusing geometry and pump energies (20 and 40 mJ), we detected the Stokes energies with different object locations. Changing the location from 18 to 80 cm, we got Stokes energy data, as shown in Fig. 3(a). The dependence of Stokes energy on location was fitted based on the experimental data. By differentiating fitting curves, one can determine the object location by peak position (Fig. 3(b)). For the pump energy of 20 mJ, the object location is at 27.8 cm; for the pump energy of 40 mJ, it is at 26.9 cm. These results agree with each other in experimental error regime. And then, the delay time between Stokes pulse and pump

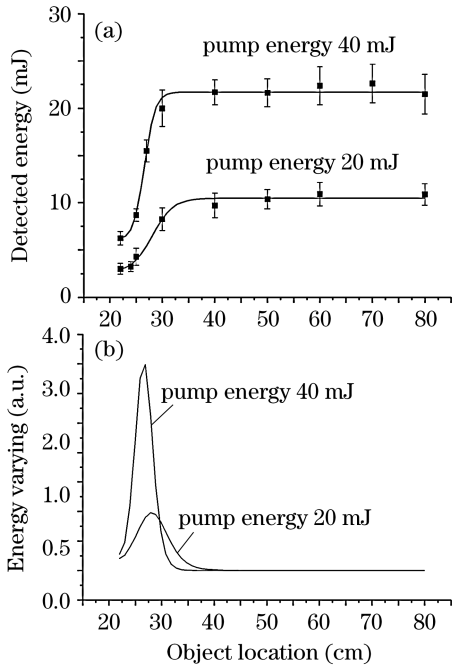

Fig. 3. Experimental data of reflected energy dependent on the object location for different pump energies.

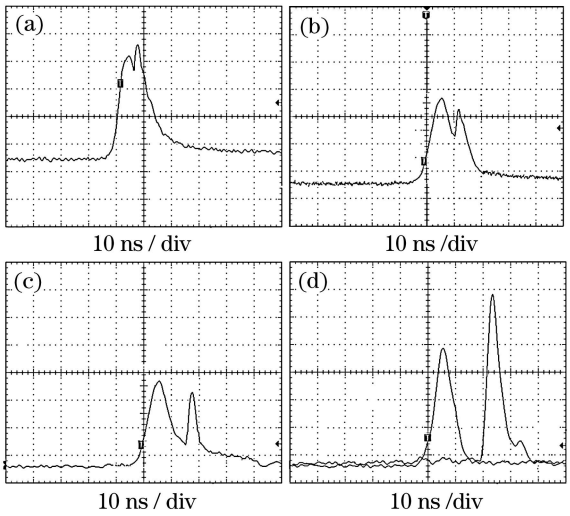

Fig. 4. Detected pulses with different locations of object. (a) $L = 30$ cm; (b) $L = 67$ cm; (c) $L = 130$ cm; (d) $L = 200$ cm.

pulse can give the object position. By the delay time, we can detect the object location in the end. The experimental results are shown in Fig. 4. In each waveform in Fig. 4, the left peak is the pump pulse that first reaches the detector, and the right is the Stokes wave that arrives later. It can be seen that the pulse width of the Stokes pulse is obviously shorter than that of the pump pulse, because the interaction between them has resulted in the pulse-narrowing effect. From Fig. 4, it is obviously seen that with the distance of the object increasing, the delay time between the two pulses increases, through $d = \frac{c\Delta t}{2n}$, the location of the object can be calculated, with Δt being the delay time between Stokes and pump waves. The results are shown in Table 1, from which it can be seen that the maximum error within the 2-m detecting range is less than 10 cm. Because the detection error

Table 1. Distances Calculated from Detected Delay Time

Δt (ns)	d_0 (cm)	d (cm)	E (cm)	RE (%)
2.9	30	32.6	2.6	8.6
3.8	40	42.7	2.7	6.8
6.2	67	69.8	2.8	4.2
7.6	8.4	85.5	1.5	1.5
9.8	104	111.0	7.0	6.7
12.1	130	136.3	6.3	5.2
18.1	200	203.8	3.8	1.9

Δt: delay time; d_0: practical distance; d: calculated distance; E: error; RE: relative error.

relies on the laser pulse width, the response speed of the electro-photonic detector and the sampling rate of the oscilloscope, it will not increase with the distance increasing evidently.

The actual detecting distance can be affected by the laser pulse energy, the emission beam diameter and the absorption of the seawater. With a large emission beam diameter and a high laser pulse energy, the laser power density will be high and the detectable distance will be long. Combining laser scanning technology, through a planar scanning of the submerged objects, not only the information of the location and the depth of the submerged objects, but also the information of their shapes can be obtained.

In conclusion, the feasibility of submerged objects detection based on SBS is validated both theoretically and experimentally in this paper. Stokes properties of SBS process within single cell focusing geometry are studied. We demonstrate the feasibility of detecting submerged objects by positions as focus in SBS process in a 2-m cell. There is a long way to go before practical applications, but we believe that the result presents the possibility for further applications in the area of submerged object detection.

This work was supported by the China Postdoctoral Science Foundation (No. 20060400230) and the Foundation for Innovation Talents by the Technology Ministry of Harbin (No. 2006RFQXG025). Y. Lü's e-mail address is luyuelan1968@163.com.

References

1. D. A. Leonard, B. Caputo, and F. E. Hoge, Appl. Opt. **18,** 1732 (1979).
2. J. G. Hirschberg J. D. Byrne, Proc. SPIE **489,** 270 (1984).
3. E. S. Fry, Y. Emery, X. Quan, and J. W. Katz, Appl. Opt. **36,** 6887 (1997).
4. J. G. Hirschberg, J. D. Byrne, A. W. Wouters, G. C. Boyton, Appl. Opt. **23,** 2624 (1984).
5. D. Liu, J. Xu, H. Wang, and J. Zhou, Proc. SPIE **4222,** 114 (2000).
6. E. S. Fry, J. Katz, D. Liu, and T. Walther, J. Mod. Opt. **49,** 411 (2002).
7. D. Liu, J. Xu, R. Li, R. Dai, and W. Gong, Opt. Commun. **203,** 335 (2002).
8. W. Gong, R. Dai, Z. Sun, X. Ren, J. Shi, G. Li, and D. Liu, Appl. Phys. B **79,** 635 (2004).
9. J. Xu, R. Dai, W. Gong, X. Ren, and D. Liu, Appl. Phys. B **79,** 131 (2004).
10. C. L. Korb, B. M. Gentry, and C. Y. Weng, Appl. Opt. **31,** 4201 (1992).
11. R. Chu, M. Kanefsky, and J. Falk, Appl. Phys. **71,** 4653 (1992).
12. R. W. Boyd, K. Rzążewski, and P. Narum, Phys. Rev. A **42,** 5514 (1990).
13. R. Chu, M. Kanefsky, and J. Falk, J. Opt. Soc. Am. B **11,** 331 (1994).
14. N. F. Andreyev, E. A. Khazanov, O. V. Palashov, and G. A. Pasmanik, J. Opt. Soc. Am. B **11,** 786 (1994).
15. Z.-W. Lü, Y.-L. Lü, and J. Yang, Chin. Phys. (in Chinese) **12,** 507 (2003).
16. B. Ya. Zel'dovich, V. I. Popovichev, V. V. Ragulskii, and F. S. Faizullov, JETP Lett. **15,** 109 (1972).
17. Y. Ding, S. Zhang, Z. Lü, and W. He, Proc. SPIE **4914,** 344 (2002).